Spot size, depth-of-focus, and diffraction ring intensity formulas for truncated Gaussian beams

Hakan Urey

Simple polynomial formulas to calculate the FWHM and full width at $1/e^2$ intensity diffraction spot size and the depth of focus at a Strehl ratio of 0.8 and 0.5 as a function of a Gaussian beam truncation ratio and a system *f*-number are presented. Formulas are obtained by use of the numerical integration of a Huygens–Fresnel diffraction integral and can be used to calculate the number of resolvable spots, the modulation transfer function, and the defocus tolerance of optical systems that employ laser beams. I also derived analytical formulas for the diffraction ring intensity as a function of the Gaussian beam truncation ratio and the system *f*-number. Such formulas can be used to estimate the diffraction-limited contrast of display and imaging systems.

OCIS codes: 110.3000, 120.2040, 120.5800, 170.5810, 260.1960, 350.5730.

1. Introduction

The characteristics of focused Gaussian beams play an important role in the design of optical systems that employ lasers, such as various laser scanning display and imaging systems[1,2] and certain layered and page-oriented optical storage architectures.[3,4] The amount of beam truncation at hard apertures is an important system design parameter that determines the radial and axial size of focused Gaussian beams and has been extensively studied in the literature with numerical methods by direct integration of the diffraction integral[5–9] or by analytic methods by use of a slowly converging infinite series of expansions.[10–14]

Prior research in this area focused mainly on developing formulas for the estimation of the shape and the encircled energy of the central main lobe, the location of the peak axial irradiance, and the location of the diffraction ring minimums and maximums. Mahajan[5,6] derived exact analytical formulas for the axial intensity of focused Gaussian beams and obtained numerical results for the encircled energy in the presence of obscurations and aberrations. Li[7] and Yura[8] derived numerical formulas for the minimum and maximum points for diffraction ring irradiance at the focal plane. More recently, Nourrit[13] derived piecewise analytical expressions for the truncated Gaussian beams in the Fresnel and Fraunhofer regime using asymptotic expansions and calculated the shape and the extrema locations of diffraction rings using finite summation formulas. Drege[14] found a closed-form expression for the far-field divergence angle.

In this paper I first derive two sets of simple polynomial formulas to calculate the width (rather than the shape) of the focused spot and the depth of focus as a function of beam truncation and the *f*-number of the focusing geometry. First, I derive polynomial formulas for the size of the focused spot using FWHM and full-width at $1/e^2$ irradiance criterion. Second, I calculate the depth of focus along the optical axis where the axial irradiance drops to 80% and 50% of the focal-plane axial irradiance.

Nourrit[13] and others listed in his references tried several methods to obtain analytical formulas to determine the minima of the diffraction rings for truncated Gaussians, but a closed-form expression cannot be found. I derived simple analytical formulas to estimate the peak and average diffraction ring irradiance as a function of Gaussian beam truncation. Diffraction ring minima are then solved numerically for different values of truncation to provide a complete solution for the irradiance profile of diffraction rings.

The formulas given in this paper can be utilized in designing various laser imaging systems for display, image capture, target tracking, microscopy, optical storage, and laser printing applications. Spot-size

H. Urey (hurey@ku.edu.tr) is with the Department of Electrical Engineering and Optoelectronics Research Center, Koç University, Sariyer, 34450 Istanbul, Turkey.

Received 8 August 2003; revised manuscript received 30 September 2003; accepted 14 October 2003.

0003-6935/04/030620-06$15.00/0

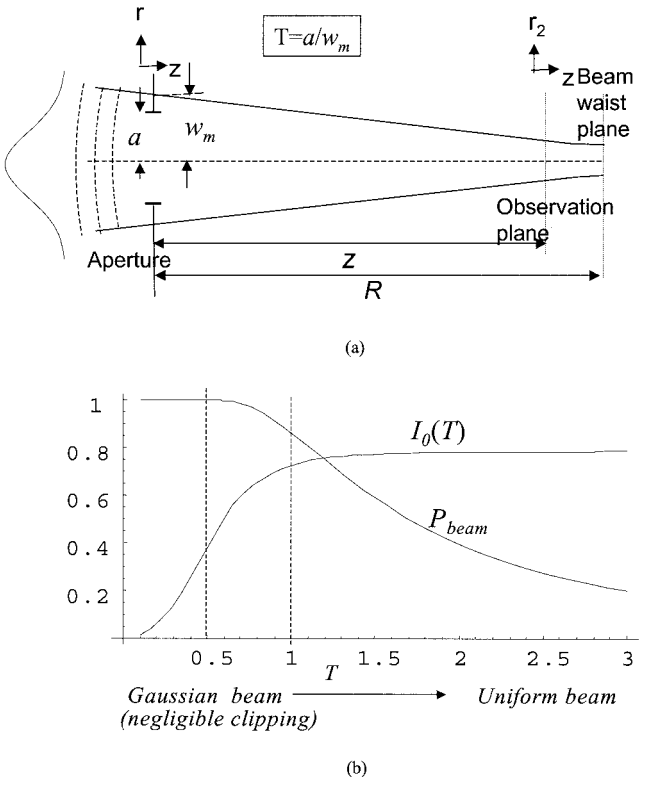

Fig. 1. (a) Schematic of converging Gaussian beam truncated by a hard aperture; (b) Power loss at the aperture and peak focal plane irradiance as a function of T.

and depth-of-focus formulas are useful for determining system resolution, modulation transfer function, and field curvature tolerance, and the diffraction ring intensity formulas are useful in determining the diffraction-limited contrast of display and imaging systems. In Section 5, I discuss the tradeoffs presented by the choice of the beam truncation ratio in an optical system design.

2. Gaussian Beam and Diffraction Integral

Consider a unity-power converging Gaussian beam, illustrated in Fig. 1(a), incident on a circular aperture (located at the exit pupil of the imaging system). The beam waist for the unclipped beam is located at a distance R behind the aperture. The modulus of the complex wave amplitude of the Gaussian beam (without the quadratic phase factor) before the aperture can be expressed as

$$|U(r, w_m)| = \sqrt{\frac{2}{\pi}}\frac{1}{w_m}\exp\left(-\frac{r^2}{{w_m}^2}\right), \quad (1)$$

where r is the radial distance from the optical axis and w_m is the beam radius. Using Eq. (1), the beam power transferred from a circular aperture of radius a can be calculated as

$$P_{\text{beam}} = 1 - \exp(-2a^2/{w_m}^2) = 1 - \exp(-2/T^2), \quad (2)$$

where $T = w_m/a$ is the Gaussian beam truncation ratio, defined as the ratio of the aperture radius to the Gaussian beam $1/e$ amplitude (or $1/e^2$ irradiance) radius at the aperture. The irradiance ($I = |U|^2$) at the far field can be calculated by use of the Huygens–Fresnel diffraction integral with the Fresnel approximations:[6,9]

$$I(T, r_2, z) = \left|\int_0^a \frac{2\pi}{\lambda z}|U(r, w_m)|\exp\left[\frac{i\pi r^2}{\lambda}\left(\frac{1}{z} - \frac{1}{R}\right)\right]J_o\left(\frac{2\pi r r_2}{\lambda z}\right)r\mathrm{d}r\right|^2, \quad (3)$$

where λ is the wavelength, R is the distance from the aperture to the Gaussian focal plane where the waist is located, z is the distance from the aperture to the observation plane, and r_2 is the radial distance from the optical axis in the observation plane. The Fresnel approximation used to obtain the above integral is valid when $z \gg a$ and $z \gg r_2$, which impose far-field and paraxial conditions.[15] Typical optical system parameters for different applications are given in Table 1. Note that far-field and paraxial conditions are satisfied for the imaging systems specified in the table.

Mahajan[5] showed that the peak axial irradiance near the focal plane shifts toward the clipping aperture, and the amount of shift is a function of the Fresnel number, which is defined as $N = a^2/\lambda R$ and is a measure of the importance of diffraction effects in the beam due to the clipping aperture (e.g., a small Fresnel number indicates greater effects of diffraction). Location of the peak axial irradiance shifts by more than 5% for systems with small Fresnel numbers ($N < 5$). However, for small Fresnel numbers, a system with a small aperture and a large focus distance compared with λ, such as Case 3 in Table 1, the depth of focus becomes very large, and the focused spot size and the encircled energy within a radius r_2 for $r_2 > \lambda R/a$ become insensitive to the shift of the peak axial irradiance position.[5,6] Therefore focused spot size can be determined with the irradiance distribution at the geometrical focal plane for all

Table 1. Optical System Parameters for Three Exemplary Optical Imaging Systems for Different Applications Assuming $T = 1$[a]

Application	Case 1 Scanning Display	Case 2 Imaging	Case 3 Projection/ Target Tracking
a (mm)	0.5	5	1
λ (nm)	635	635	635
R (mm)	80	20	2000
N	5	1969	1
$f_\#$	80.0	2.0	1000.0
FWHM spot size s_{fwhm} (μm)	57.6	1.4	720.1
Depth of focus − Δ (mm)	9	0.005	1340
R/Δ − ratio	9.3	3731.8	1.5
R_2 (mm) for $r_n = 20$	1.016	0.0254	12.7

[a]Table 2 formulas are used to calculate the spot size and the depth of focus.

Fresnel-number and beam-truncation ratios encountered in imaging systems (except for the case when the aperture size is not much larger than λ, which is not of interest for the imaging applications considered here). I therefore neglect the focus shift and determine the spot size by turning attention to the irradiance distribution at the Gaussian focal plane (i.e., $z = R$).

I simplify the math by using the following normalized variables: $f_{\#} = R/(2a)$ is the focal ratio of the focusing geometry, $\rho = r/a$ is the normalized aperture coordinate, and $r_n = r_2/\lambda f_{\#}$ is the normalized radial focal-plane coordinate. After substituting the variables in Eq. (3) and normalizing the irradiance with P_{beam}, the diffraction integral for points near the focal plane can be rewritten as

$$I(T, r_n, z) = \frac{8\pi a^2}{\lambda^2 z^2 T^2 P_{\text{beam}}} \left| \int_0^1 \exp(-\rho^2/T^2) \exp\underbrace{\left[\frac{i\pi\rho^2 a^2}{\lambda} \left(\frac{1}{z} - \frac{1}{R} \right) \right]}_{\frac{i\pi\rho^2 N \Delta z}{z}} J_o\left(\frac{\pi \rho r_n R}{z} \right) \rho \, d\rho \right|^2, \tag{4}$$

where $\Delta z = R - z$ is the defocus. The diffraction integral at the focal plane (i.e., $z = R$) simplifies to

$$I_{\text{focal}}(T, r_n) = \frac{2\pi}{\lambda^2 f_{\#}^2 T^2 P_{\text{beam}}} \times \left| \int_0^1 \exp(-\rho^2/T^2) J_o(\pi \rho r_n) \rho \, d\rho \right|^2. \tag{5}$$

The axial irradiance (I_o), which is the peak irradiance for an arbitrary T and for uniform beam illumination ($T \to \infty$) are found by substituting $r_n = 0$:

$$I_0(T) = \frac{\pi T^2 [1 - \exp(-1/T^2)]^2}{2\lambda^2 f_{\#}^2 [1 - \exp(-2/T^2)]},$$

$$I_0(T \to \infty) = \frac{\pi}{4\lambda^2 f_{\#}^2}. \tag{6}$$

Figure 1(b) shows the beam power and the peak irradiance given in Eqs. (2) and (6) as a function of T. As T increases, the power loss at the aperture increases. If the power is normalized with the power transferred from the aperture, then the peak axial irradiance increases with T and reaches maximum for uniform illumination. If the power is normalized with the incident power, then the optimal truncation ratio that gives the peak axial irradiance is around $T = 0.9$ (Ref. 11). This result is not really significant in an imaging system, since the width of the focused spot and the encircled energy is far more important than the peak axial irradiance.

An analytical formula for the beam irradiance along the optical axis as a function of defocus $\Delta z = R - z$ and Fresnel number N can be obtained by setting $r_n = 0$ in Eq. (4) (integration is carried out by use of MATHEMATICA™ by Wolfram Research, Inc., Champaign, Ill.):

$$I_{\text{axial}}(T, z) = \frac{2\pi a^2 T^2 \left[\coth(1/T^2) - \cos\left(\frac{\pi N \Delta z}{z} \right) \Big/ \sinh(1/T^2) \right]}{\lambda^2 z^2 \left(1 + \frac{\pi^2 T^4 N^2 \Delta z^2}{z^2} \right)}. \tag{7}$$

For small N, I_{axial} is not symmetrical on either side of the focus, and as discussed above, the peak axial irradiance shifts toward the aperture. Mahajan[15] discusses the properties of I_{axial} in more detail.

3. Focal Plane Spot Size and Depth of Focus

For a converging beam truncated at a circular aperture, the focused beam profile is Gaussian for $T < 0.5$ and converges to the Airy pattern as $T \to \infty$. One can define a diffraction spot diameter (s) on the basis of a certain fraction of the peak irradiance, such as 0.5 or $1/e^2$. The corresponding r_n can be solved by setting the ratio of I_{focal} to I_0, given in Eqs. (5) and (6), equal to a constant. If the constant used is larger than the maximum diffraction ring intensity, one can find a unique solution for r_n within the central lobe of the irradiance profile as a function of T. Since r_n is normalized with $\lambda f_{\#}$, the focal plane spot size (s) can be expressed as

$$s = K \lambda f_{\#}, \tag{8}$$

where K is the spot size constant that is a function of beam truncation only and is independent of other system parameters. The paraxial approximation limits the validity of this formula to $f_{\#} > 2$. An alternative form of this formula is to express the spot size as $s = 0.5K\lambda/(\text{NA})$, where NA is the numerical aperture of the system. This alternative form is more accurate for $f_{\#} < 2$, such is the case in lithography or microscopic imaging systems.

Similarly, one can find Δz, where I_{axial} becomes a certain fraction of I_0, such as 0.8 or 0.5. Equations (4) and (7) reveal that, if I_{axial}/I_0 ratio is set equal to a constant, for each particular value of T, the solution to the equation yields a constant value for the term $N\Delta z/z$ ratio. Therefore I can express Δz as a function of z/N. Furthermore, when the defocus is small compared with the focus distance (i.e., $\Delta z < R$), Δz can be written as proportional to $\lambda f_{\#}^2$, as follows:

$$\Delta z = K_2 z/4N \approx K_2 \lambda f_{\#}^2, \tag{9}$$

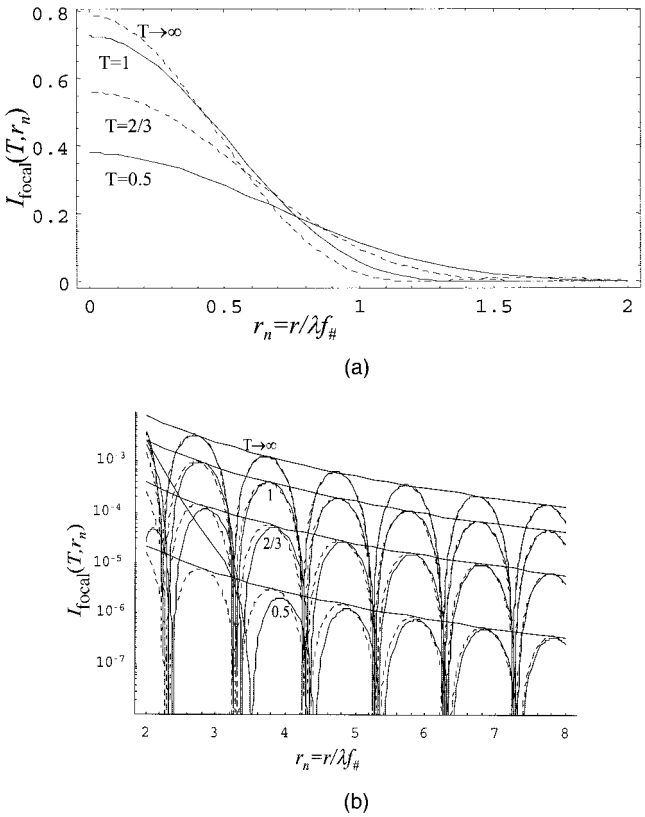

Fig. 2. Focal plane irradiance cross sections for different Gaussian beam truncation ratios assuming unity total power beam. (a) Irradiance for $r_n < 2$, (b) Irradiance in log scale for $r_n > 2$. Solid curves are numerical solution of Eq. (5) normalized by the beam power transferred from the aperture, and dashed curves are approximate analytical solutions of Eqs. (12) and (13). Peak ring irradiances are also shown.

where K_2 is the depth-of-focus constant that is a function of beam truncation only and is independent of other system parameters. The approximation in the above figure is valid in systems where $N < 5$ (e.g., K_2 formulas are not valid for Case 3 in Table 1). For systems where $N < 5$, the axial irradiance profile is not symmetrical around the geometric focus, and the maximum axial irradiance shifts from the geometric focal plane towards the aperture. Other system parameters play a role, and the $\Delta z = K_2 \lambda f_\#^2$ approximation is no longer valid. The depth of focus can be calculated directly by use of Eq. (7). However, in such systems the depth of focus is large enough that one need not worry about effects of defocusing.

Figure 2 shows the numerical simulation results obtained with Eq. (5) and illustrates how the spot profile, the peak irradiance, the spot width, and the energy shifted to the diffraction rings change with T.

Table 2 is a summary of my results in this section and shows the simple formulas for the diffraction-limited spot diameter coefficient K and the depth of focus coefficient K_2. The table formulas are obtained by polynomial curve fitting to the numerical solutions of Eqs. (5) and (7). K is calculated for two commonly used spot-size criteria in imaging systems: full width at $1/e^2$-irradiance (FWE2) and FWHM irradiance. K_2 is calculated for a Strehl Ratio (SR) of 0.8 and a SR of 0.5 cases, where SR is defined as the ratio of the axial irradiance at the observation plane to the peak axial intensity at the focal plane. SR = 0.5 corresponds to the Rayleigh range for a Gaussian beam, and SR = 0.8 corresponds to the diffraction-limited range of a beam in imaging systems. The depth-of-focus formulas in Table 2 can be used to compute the depth of a page in a page-oriented three-dimensional optical memory or the depth-of-focus and the field-curvature aberration tolerance of a scanning display or imaging system.

Drege[14] gives an analytical expression for the far-field divergence angle of a truncated Gaussian beam. By use of Drege's result and after some algebra, the following analytical formula for the FWE2 irradiance spot-size coefficient can be obtained:

$$K_{\mathrm{FWE2}} = \frac{0.97}{T}\left[\frac{e}{1-\exp(-1/T^2)} - 1\right]^{1/2}. \quad (10)$$

Figure 3 illustrates the K factor as a function of T, using the formulas in the first row of Table 2. My empirical formulas for FWE2 and FWHM irradiances are within 1%, and Drege's approximate FWE2 for-

Table 2. Spot Size and Depth-of-Focus Formulas as a Function of Truncation Ratio *T*. *K* and K_2 for *T* < 0.5 Are Calculated by Use of Standard Gaussian Beam Formulas

$T = w_m/a$ $f_\# = R/2a$	$T < 0.5$ (Gaussian)	$T > 0.4$ (Truncated Gaussian) [Error < 1%]
Spot Size $s = K\lambda f_\#$		
full width at $1/e^2$ irradiance	$K_{\mathrm{FWE2}} = \dfrac{1.27}{T}$	$K_{\mathrm{FWE2}} = 1.654 - \dfrac{0.105}{T} + \dfrac{0.28}{T^2}$
full width at 50% irradiance	$K_{\mathrm{FWHM}} = \dfrac{0.75}{T}$	$K_{\mathrm{FWHM}} = 1.036 - \dfrac{0.058}{T} + \dfrac{0.156}{T^2}$
Depth of Focus $\Delta z = K_2 \lambda f_\#^2$		
K_2 for Strehl Ratio = 0.5	$K_{2,\mathrm{SR}=0.5} = \dfrac{1.27}{T^2}$	$K_{2,\mathrm{SR}=0.5} = 3.5 + \dfrac{0.33}{T} - \dfrac{0.73}{T^2} + \dfrac{0.52}{T^3}$
K_2 for Strehl Ratio = 0.8	$K_{2,\mathrm{SR}=0.8} = \dfrac{0.635}{T^2}$	$K_{2,\mathrm{SR}=0.8} = 2.05 + \dfrac{0.12}{T} - \dfrac{0.28}{T^2} + \dfrac{0.22}{T^3}$

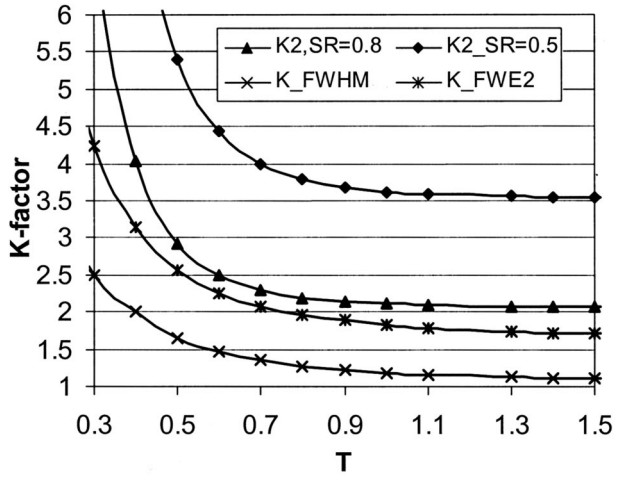

Fig. 3. Spot-size constant and the depth-of-focus constants as a function of T by use of the formulas in Table 1.

mula is within 3% of the numerical integration results. As N and $f_{\#}$ become larger, the formulas have better accuracy.

4. Diffraction Ring Irradiance

I derive analytical formulas for estimating the diffraction ring irradiance for points away from the optical axis (large r_n) as a function of T. Closed-form simple expressions for the diffraction ring peak irradiance cannot be found elsewhere in the literature.

The following approximation can be used for the Bessel function in Eq. (5) for large values of x[16]

$$J_o(x) \approx \sqrt{2/\pi x}\,\cos(\pi/4 - x). \tag{11}$$

Figure 4(a) shows the integrand in Eq. (5) and its approximation by use of Eq. (11) for an exemplary case of $T = 1$. The figure illustrates that the approximation is indeed a good one for $r_n \gg 1$. Note that when $r_n \gg 1$ the integrand in Eq. (5) alternates sign approximately r_n times between the limits of integration. Owing to the large number of oscillations, the value of the integral crosses zero many times, the last one being near $\rho = 1$. Therefore we can approximate the integral by moving the exponential term outside the integral by substituting $\rho = 1$ for that term. The integrands in exact form and in approximate form can then be written as

$$\text{Integrand\_exact} = \int_0^1 \exp(-\rho^2/T^2) J_o(\pi\rho r_n)\rho\,d\rho,$$

$$\text{Integrand\_approx} = \exp(-1/T^2)\sqrt{\frac{2}{\pi^2 r_n}}\int_x^1 \cos(\pi/4 - \pi\rho r_n)\,d\rho, \tag{12}$$

where x is the coordinate of the last zero crossing of the integral and depends mainly on r_n and becomes very close to 1 as r_n increases. The approximation in Eq. (12) is also supported by Fig. 4(b), which shows the results of the integrations in Eq. (12) for $T = 1$ when

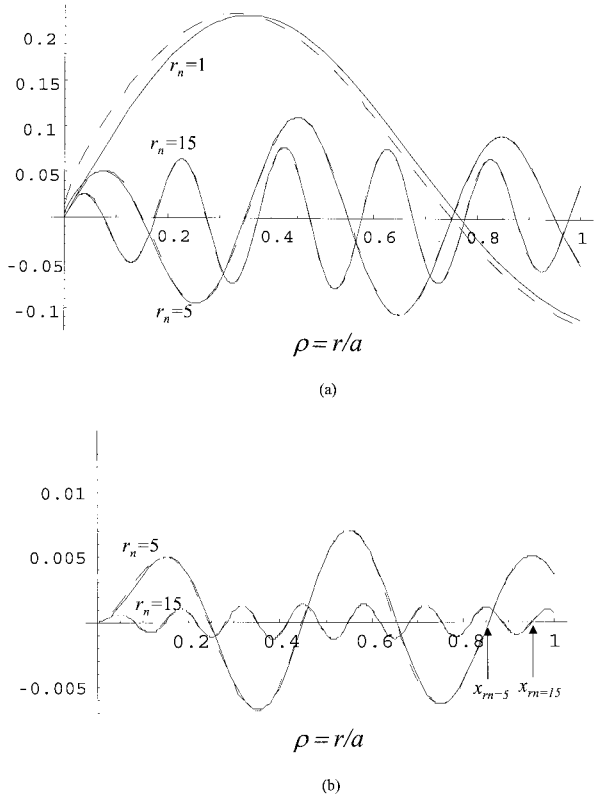

Fig. 4. (a) Integrand and the result of integration in Eq. (12) as a function of ρ for different values of r_n, with dashed curves showing the exact formula and solid curves showing the approximate formula in Eq. (12); (b) the result of the integral for the integrand in (a) with integration limit from 0 to ρ (result for $r_n = 1$ is too large and is not shown).

the limits of integrations are set from 0 to ρ. Figure 4(b) also illustrates that the location of the last zero crossing is given approximately by $x \approx 1 - 1/r_n$.

The integral in Eq. (5) can then be approximated as

$$I_{\text{focal}}(T, r_n) \approx \frac{2\pi\,\exp(-2/T^2)}{\lambda^2 f_{\#}^{\,2} T^2 P_{\text{beam}}}\left|\sqrt{\frac{2}{\pi^2 r_n}} \times \int_x^1 \cos(\pi/4 - \pi\rho r_n)\,d\rho\right|^2$$

$$\approx \frac{4\,\exp(-2/T^2)}{\lambda^2 f_{\#}^{\,2}\pi^3 r_n^{\,3} T^2 P_{\text{beam}}}\sin^2(\pi r_n - q), \tag{13}$$

where $P_{\text{beam}} = \exp(-2/T^2)$ and q is a phase factor that is a function of r_n and T. For large r_n (i.e., beyond the second zero crossing of the irradiance profile), numerically determined values of q for $T = 0.5$, $T = 0.66$, $T = 1$, and $T \to \infty$ are 1.04, 0.93, 0.84, and 0.77, respectively. Phase factor q for other T can be estimated by interpolation.

The Airy pattern for large r_n is the limit of Eq. (13) when $T \to \infty$:

$$I_{\text{focal}}(T \to \infty, r_n) \approx \frac{2\,\sin^2(\pi r_n - \pi/4)}{\lambda^2 f_{\#}^{\,2}\pi^3 r_n^{\,3}}. \tag{14}$$

Figure 2(b) shows the numerical solution of the integral in Eq. (5) (solid curves) and the approximate solution obtained by use of Eq. (13) (dashed curves). As r_n becomes larger, the dashed curves in the figure converge to the solid curves. The approximate formulas work well beyond the second zero crossing of the function. The limiting case $T \to \infty$ gives a good approximation for the Airy pattern for $r_n > 0.6$. The figure also shows the peak diffraction ring irradiances in each case. Since the average value of $\sin^2$ term in Eq. (13) is 0.5, the average diffraction ring irradiance can be written as the half of the peak irradiance:

$$I_{\text{focal,avg}}(T, r_n) = \frac{2 \exp(-2/T^2)}{\lambda^2 f_\#^2 \pi^3 r_n^3 T^2 [1 - \exp(-2/T^2)]},$$

$$I_{\text{focal,avg}}(T \to \infty, r_n) = \frac{1}{\lambda^2 f_\#^2 \pi^3 r_n^3}. \quad (15)$$

5. Discussion and Conclusions

I presented simple polynomial formulas for calculating the FWHM and FWE2 spot size and depth of focus at the SRs of 0.8 and 0.5. The spot size and depth of focus are expressed as a function of λ and $f_\#$, which greatly simplifies the optical system design problem whenever the approximation is valid. The formulas are valid when $N > 5$ and $f_\# > 2$, such as the scanning display and imaging systems listed in Table 1. For systems with a small Fresnel number ($N < 5$), such as target tracking systems or projection display systems, the depth-of-focus formulas are not valid, but the depth of focus is so large that the defocus and the field curvature aberration owing to defocus is not an issue.

I also presented a simple closed form formulas for diffraction ring irradiance using an analytical approximation to the diffraction integral shown in Eqs. (14) and (15). These equations are the simplest expressions for the numerical computation of the diffraction ring irradiance as a function of beam truncation for large r_n.

I used the formulas in Table 1 and Eq. (15) in the design of various optical systems, such as a confocal imaging system, a Retinal Scanning Display design, and two-photon absorption volumetric optical storage systems.[1–3] A range of values for typical optical system parameters used in imaging and display applications is given in Table 2. As N and $f_\#$ become larger, the formulas have better accuracy.

In most imaging systems employing Gaussian beams, the optimal aperture size (or exit pupil size) can be obtained by setting T in the range $0.4 < T < 1$. In scanning systems, such as Retinal Scanning Displays, the limiting system aperture is typically the scan mirror, and the tradeoff in choosing T is between the system resolution,[1] the power efficiency, the maximum achievable contrast,[17,18] and the display exit pupil profile that is shaped using a binary diffraction grating.[19] For $T < 0.5$, the mirror is underfilled. Clipping at the aperture is negligible, and the beam profile remains Gaussian as it propagates; however, the system resolution is poor. For $T > 1$, the mirror is overfilled, and the focused spot profile converges to an Airy pattern as $T \to \infty$, yet the power lost at the aperture and the diffraction ring intensities may be too large, limiting the diffraction-limited maximum achievable contrast of the display. $T < 0.5$ appears too conservative, and increasing T beyond 1.0 increases the power loss and reduces the maximum achievable contrast substantially without improving the resolution. As an example, increasing truncation from $T = 2/3$ to $T = 1$ increases the power loss from 1.1% to 13.5%, reduces the FWHM spot size, and increases the scanning system resolution by 13%. However, it increases the energy shifted to the diffraction rings, reducing the maximum achievable diffraction limited contrast by a factor of ~7.5.[17]

References

1. H. Urey, D. Wine, and T. Osborn, "Optical performance requirements for MEMS scanner based microdisplays," in *MOEMS and Miniaturized Systems*, M. E. Motamedi and R. Goering, eds., Proc. SPIE **4178,** 176–185 (2000).
2. G. Marshall, ed., *Optical Scanning* (Marcel-Dekker, New York, 1991).
3. H. Urey and F. B. Mccormick, "Storage limits of two-photon based three-dimensional memories," in *Optical Computing*, Vol. 8 of OSA Proceedings Series (Optical Society of America, Washington, D.C., 1997), pp. 134–136.
4. M. M. Wang, S. C. Esener, F. B. McCormick, I. Cokgor, A. S. Dvornikov, and P. M. Rentzepis, "Experimental characterization of a two-photon memory," Opt. Lett. **22,** 558–560 (1997).
5. V. N. Mahajan, "Axial irradiance and optimum focusing of laser beams," Appl. Opt. **22,** 3042–3053 (1983).
6. V. N. Mahajan, "Uniform versus Gaussian beams: a comparison of the effects of the diffraction, obscuration, and aberrations," J. Opt. Soc. Am. A **3,** 470–485 (1986).
7. Y. Li, "Degeneracy in the Fraunhofer diffraction of truncated Gaussian beam," J. Opt. Soc. Am. A **4,** 1237–1242 (1987).
8. H. T. Yura, "Optimum truncation of a Gaussian beam for propagation through atmospheric turbulence," Appl. Opt. **34,** 2774–2779 (1995).
9. H. T. Yura and T. S. Rose, "Gaussian beam transfer through hard-aperture optics," Appl. Opt. **34,** 6826–6828 (1995).
10. P. Belland and J. P. Crenn, "Changes in the characteristics of a Gaussian beam weakly diffracted by a circular aperture," Appl. Opt. **21,** 522–527 (1982).
11. K. Tanaka, N. Saga, and H. Mizokami, "Field spread of a diffracted Gaussian beam through a circular aperture," Appl. Opt. **24,** 1102–1106 (1985).
12. G. Lenz, "Far-field diffraction of truncated higher-order Laguerre–Gaussian beams," Opt. Commun. **123,** 423–429 (1996).
13. V. Nourrit, J.-L. de Bougrenet de la Tocnaye, and P. Chanclou, "Propagation and diffraction of truncated Gaussian beams," J. Opt. Soc. Am. A **18,** 546–556 (2001).
14. E. M. Drege, N. G. Skinner, and D. M. Byrne, "Analytical far-field divergence angle of a truncated Gaussian beam," Appl. Opt. **39,** 4918–4925 (2000).
15. V. N. Mahajan, *Optical Imaging and Aberration Part II, Wave Diffraction Optics* (SPIE Press, Bellingham, Wash., 2001).
16. M. Abromovitz and I. A. Stegun, *Handbook of Mathematical Functions* (Dover, New York, 1972).
17. H. Urey, "Diffraction limited resolution and maximum contrast for scanning displays," Proc. Soc. Inf. Disp. **31,** 866–869 (2000).
18. G. de Wit, "Contrast budget of head mounted displays," Opt. Eng. **41,** 2419–2426 (2002).
19. H. Urey, "Diffractive exit-pupil expander for display applications," Appl. Opt. **40,** 5840–5851 (2001).